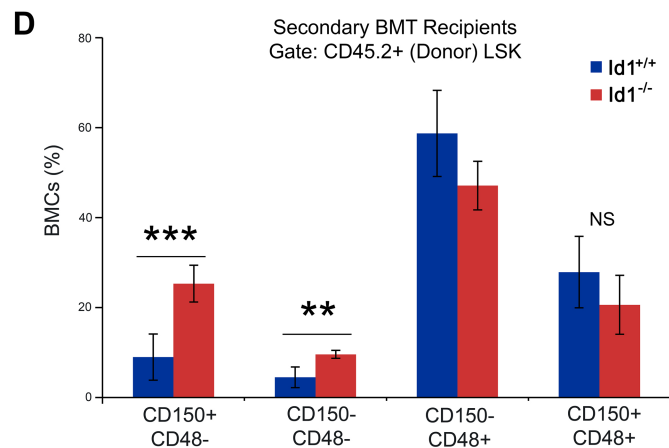
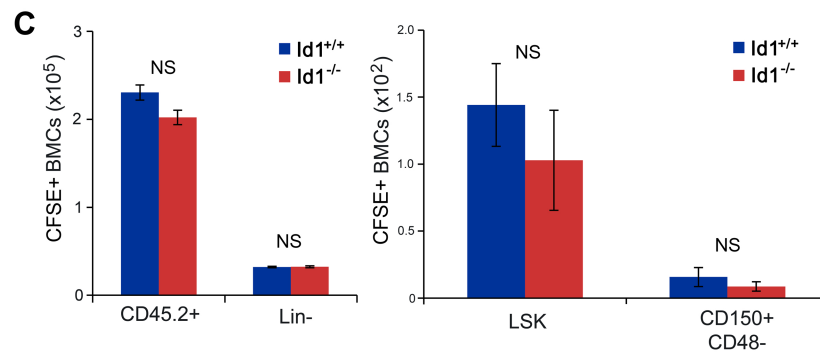
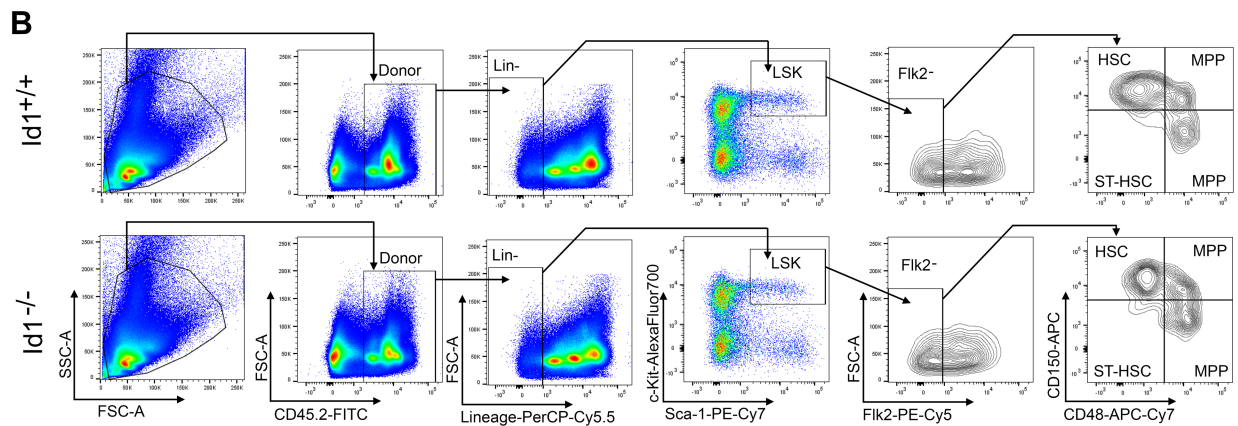
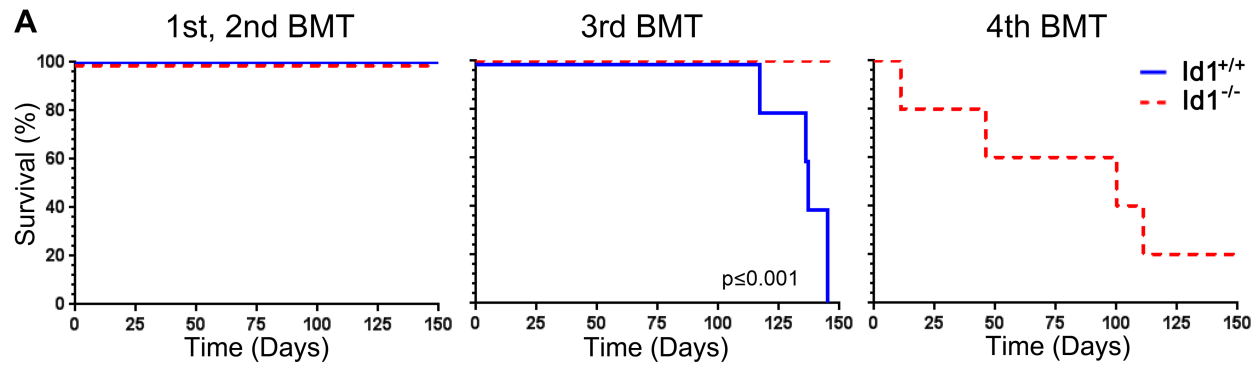


Supplemental Figure 1

Figure S1. Related to Figure 1, Effect of Id1 loss on hematopoietic stem and progenitor cell development and differentiation in mice on a C57BL/6 background.

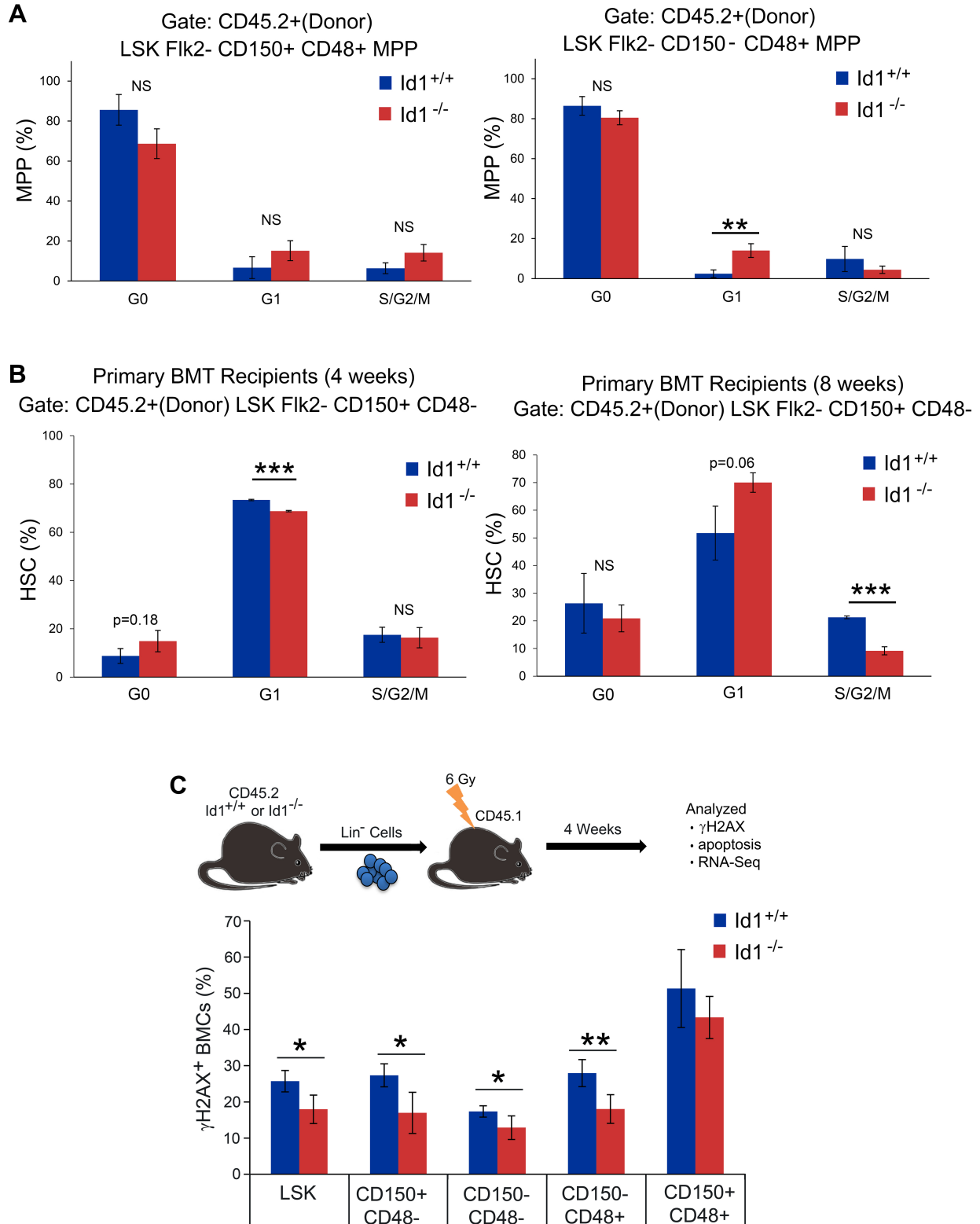
(A) $Id1^{-/-}$ mice were backcrossed to C57BL/6 mice for 10 generations and analyzed for hematopoietic lineage development by flow cytometry. Percentage of B cells ($B220^{+}$), T cells ($CD4^{+}$ and $CD8^{+}$) and neutrophils ($Mac-1^{+}Gr-1^{+}$) in the peripheral blood of 8-week-old C57BL/6 $Id1^{+/+}$ and $Id1^{-/-}$ mice (n=5 mice/group). Data are presented as mean \pm SD, and are representative of two independent experiments. (B) Percentage of B cells ($B220^{+}$) and neutrophils ($Mac-1^{+}Gr-1^{+}$) in the bone marrow of 8-week-old C57BL/6 $Id1^{+/+}$ and $Id1^{-/-}$ mice (n=5). Data are presented as mean \pm SD, and are representative of two independent experiments. (C) Total bone marrow cellularity of 8-week-old C57BL/6 $Id1^{+/+}$ and $Id1^{-/-}$ mice (n=5). Data are presented as mean \pm SD, and are representative of two independent experiments. (D) Flow cytometry analysis of BMCS from 8-week-old C57BL/6 $Id1^{+/+}$ and $Id1^{-/-}$ mice for HSPCs. The gating strategy for HSCs ($LSK CD150^{+}CD48^{-}$), ST-HSCs ($LSK CD150^{-} CD48^{-}$), and MPPs ($LSK CD150^{-} CD48^{+}/LSK CD150^{+}CD48^{+}$) is shown. (E) Total number of HSPCs in 8-week-old C57BL/6 $Id1^{+/+}$ and $Id1^{-/-}$ mice (n=5). HSPC numbers were determined from the percentages of HSPC by flow cytometry, and total BM cellularity, using the gating strategy shown in Figure S1D. Data are presented as mean \pm SD, and are representative of two independent experiments. (F) Summary of hematopoietic development in $Id1^{+/+}$ and $Id1^{-/-}$ mice on C57BL/6 background (red arrows), and previously reported B6;129 mixed background (blue arrows).



Supplemental Figure 2

Figure S2. Related to Figure 1, Enhanced self-renewal of *Id1*^{-/-} BMCs in noncompetitive bone marrow transplantation assays.

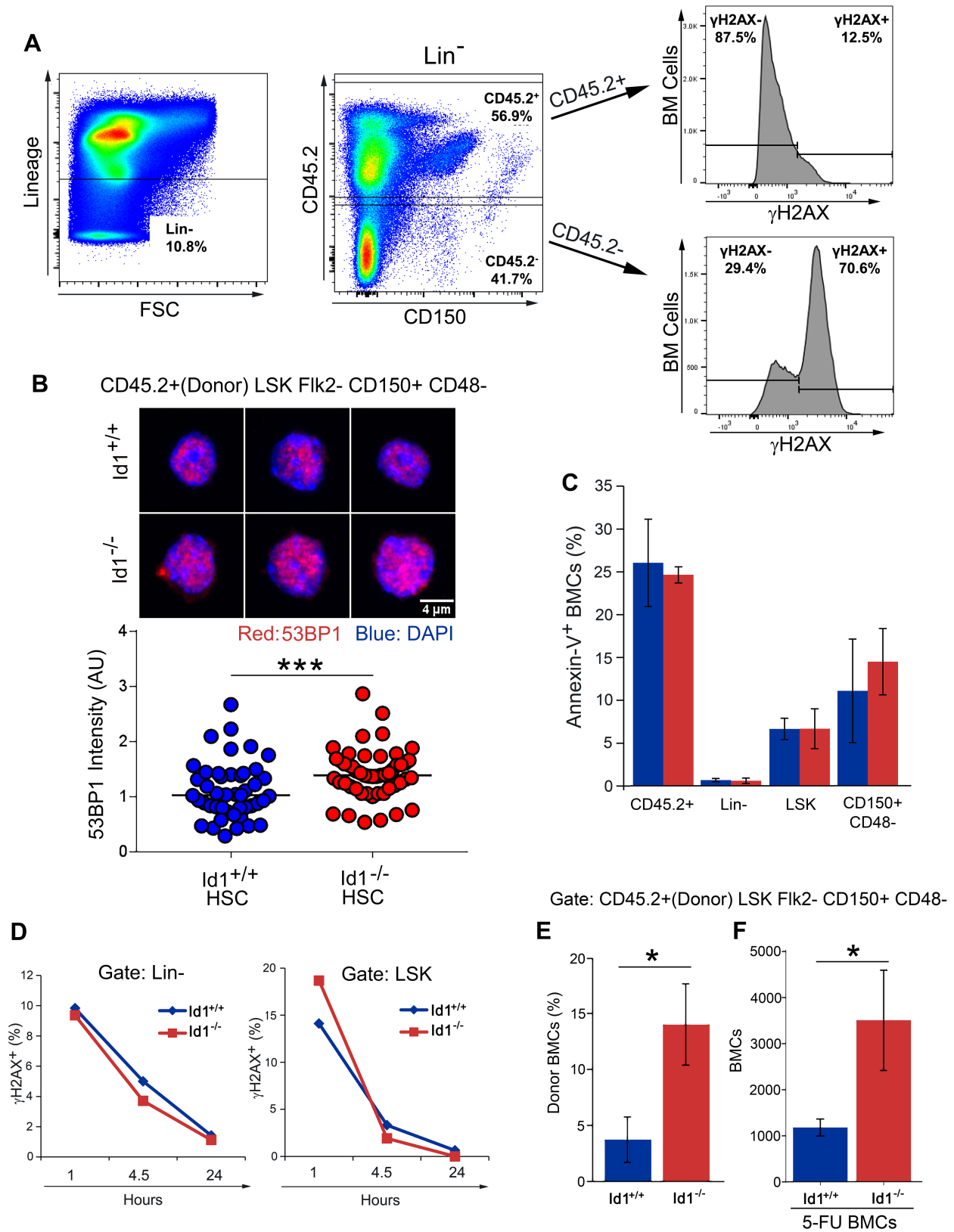
(A) Kaplan-Meier analysis of the survival of primary, secondary, tertiary and quaternary non-competitive BMT recipient mice. CD45.2⁺ BMC (1×10^6) from *Id1*^{+/+} and *Id1*^{-/-} mice were transplanted into 10 Gy irradiated CD45.1⁺ recipient mice (n=5 mice/group, Mantel-Cox test P=0.0001). BMCs were harvested from mice 20 weeks after BMT, and pooled BMCs were serially transplanted (1×10^6 BMCs/mouse) under the same conditions. These data are representative of two independent experiments. (B) Flow cytometry analysis of BMCS 12 weeks after the primary BMT of *Id1*^{+/+} and *Id1*^{-/-} mice for HSPCs. The gating strategy for HSCs (CD45.2⁺ Donor LSK CD150⁺CD48⁻), ST-HSCs (CD45.2⁺ Donor LSK Flk2⁻CD150⁻CD48⁻), and MPPs (CD45.2⁺ Donor LSK Flk2⁻CD150⁻CD48⁺ and CD45.2⁺ Donor LSK Flk2⁻CD150⁺CD48⁺) is shown. (C) *Id1*^{+/+} and *Id1*^{-/-} progenitor cells show similar bone marrow homing ability. CFSE labeled *Id1*^{+/+} and *Id1*^{-/-} Lin⁻ BMCs (2×10^6) were transplanted into 8 Gy irradiated CD45.1 recipients. After 2.5 days BMCs were harvested and the number of donor-derived CFSE⁺ HSPCs was determined by flow cytometry using the gating strategy shown in Figure S2B without Flk2 antibodies (n=5 mice/group). The data are presented as the mean \pm SD. (D) Loss of Id1 does not affect MPP development in secondary BMT recipient mice. BMCs from primary competitive recipient mice were pooled and transplanted into secondary recipient mice. BMCs were harvested from secondary competitive BMT recipients after twelve weeks, and analyzed for donor-derived HSPC development using the gating strategy shown in Figure S2B without Flk2 antibodies. The data are presented as mean \pm SD, **P < 0.01, ***P < 0.001, and are representative of three independent experiments.



Supplemental Figure 3

Figure S3. Related to Figure 2, Reduced cycling and γ H2AX phosphorylation of $Id1^{-/-}$ HSCs following bone marrow transplantation.

(A) $Id1^{+/+}$ and $Id1^{-/-}$ MPPs show similar levels of cell cycling in primary recipient mice. BMCs were harvested from mice 12 weeks after competitive transplantation of $Id1^{+/+}$ and $Id1^{-/-}$ BMC, and then analyzed for HSPCs and cell cycle using Ki-67/FxCycle by flow cytometry as described in Experimental Procedures, using the gating strategy shown in Figure S2B. Percentage of donor-derived MPPs (LSK Flk2⁻CD150⁻ CD48⁺ and LSK Flk2⁻150⁺48⁺) in G0/G1/S/G2M is shown for primary recipient mice (n=5 mice/group). Data are representative of two independent experiments. (B) Decreased cycling of $Id1^{-/-}$ HSCs in primary recipient mice. BMCs were harvested from mice 4 and 8 weeks after competitive transplantation of $Id1^{+/+}$ and $Id1^{-/-}$ BMC, and then analyzed for HSPCs using the gating strategy shown in Figure S2B, and cell cycle using Ki-67/FxCycle and flow cytometry as described in Experimental Procedures. Percentage donor HSCs (LSK Flk2⁻CD150⁺ CD48⁻) and ST-HSCs (LSK Flk2⁻CD150⁺ CD48⁻) in G0/G1/S/G2M in primary recipients is shown (n=5 mice/group). Data are representative of two independent experiments. (C) $Id1^{-/-}$ HSCs show reduced γ H2AX staining 4 weeks after BMT. Schematic of Lin⁻ BMT (upper panel). BMCs were harvested from primary recipient mice 4 weeks after transplantation of Lin⁻ BMCs (3×10^6 cells/mouse) (n=5 mice/group). The level of γ H2AX phosphorylation in donor-derived (CD45.2⁺) HSPC populations was determined by HSPC analysis and flow cytometry (lower panel) using the gating strategy shown in Figure S2B without Flk2 antibodies. Data are representative of two independent experiments. HSCs were purified from these mice by flow cytometry and RNA was isolated for RNA-seq as described in the Experimental Procedures. For all graphs, the data are presented as mean \pm SD, *P < 0.05, **P < 0.01, ***P < 0.001.



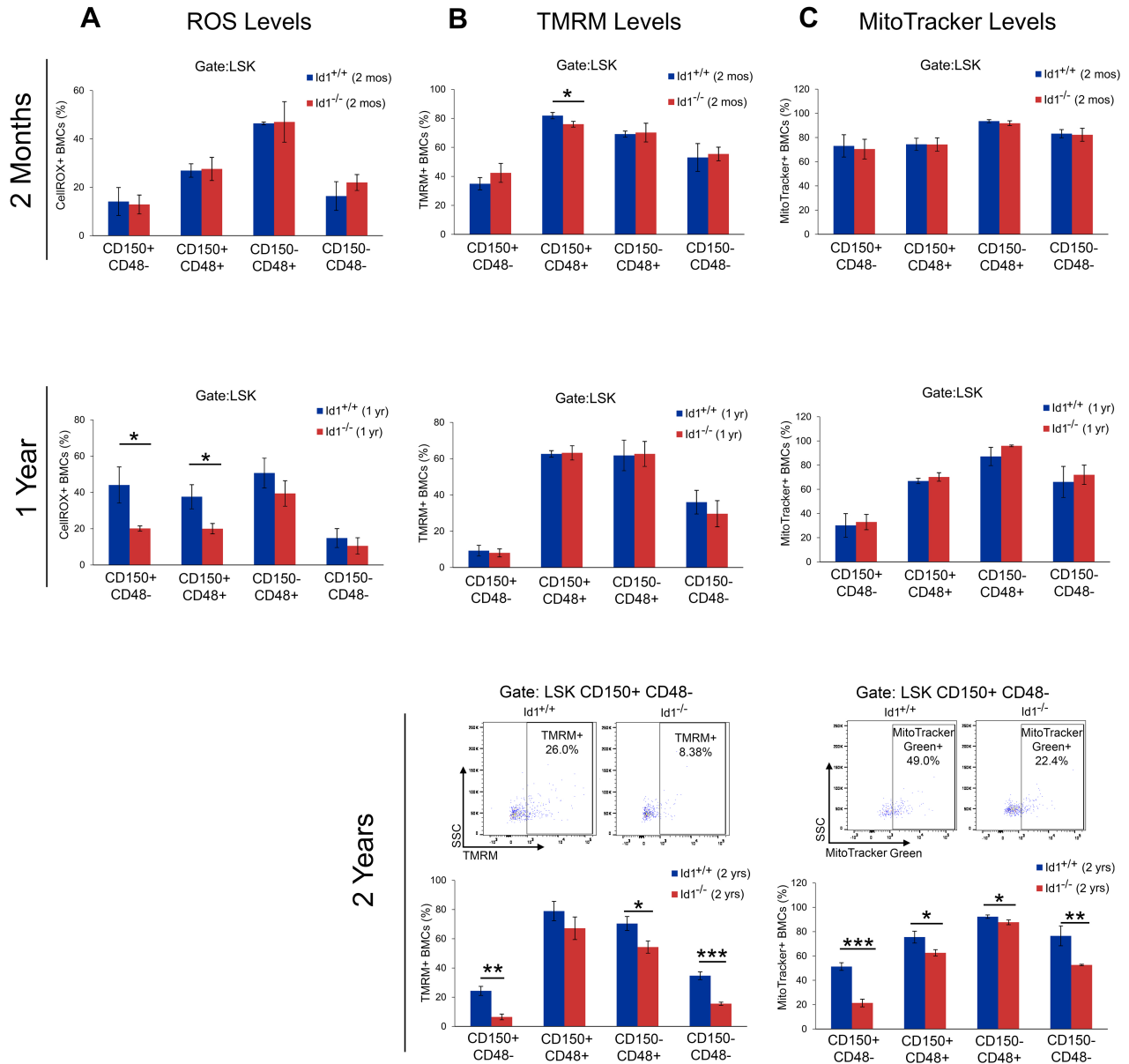
Supplemental Figure 4

Figure S4. Related to Figure 2, Expression of γ H2AX and 53BP1 in *Id1*^{-/-} HSCs.

(A) High levels of γ H2AX phosphorylation in host BMCs after γ -IR and BMT. BMCs were harvested from primary BMT recipient mice transplanted with *Id1*^{+/+} and *Id1*^{-/-} BMCs. Donor and host HSPCs were analyzed for γ H2AX phosphorylation levels by flow cytometry. Representative FACS plot of Lin⁻ gated cells (left panel), donor (CD45.2⁺) and host (CD45.2⁻) gated cells (middle panel), and histogram of γ H2AX stained cells (right panels). Percentage γ H2AX⁺ and γ H2AX⁻ for Lin⁻ donor and host BMCs are indicated. **(B)** *Id1*^{-/-} HSCs from primary BMT recipient mice show increased 53BP1 staining. BMCs were harvested from primary recipient mice 12 weeks after competitive BMT, and then donor *Id1*^{+/+} and *Id1*^{-/-} HSCs were FACS sorted and stained with antibodies that recognize 53BP1, imaged by confocal microscopy, and quantified for fluorescence according to the methods described in the Experimental Procedures. Mann-Whitney test $p < 0.0009$, and z-score 3.35. Data are representative of two independent experiments. **(C)** Loss of Id does not affect HSC survival during BMT. Percentage of donor-derived annexin V⁺ HSPCs populations after secondary BM transplantation. BMCs from primary competitive BMT recipient mice were pooled and transplanted into secondary recipient mice, and BMCs were harvested from secondary competitive BMT recipients after 12 weeks, and analyzed for donor HSPC using the gating strategy shown in Figure S2B without Flk2 antibodies, and Annexin-V⁺ cells by flow cytometry (n=5 mice/group). Data are presented as mean \pm SD, and are representative of two independent experiments. **(D)** Id1 does not have a direct role in DNA damage repair. *Id1*^{+/+} and *Id1*^{-/-} BMCs were cultured in StemSpan (SFEM) media with mSCF/hTPO (5x10⁶ cells/ml) for 16 hours, and then γ -IR with 6 Gy on ice. Cells were resuspended in pre-warmed StemSpan media, cultured for the indicated times, and assessed for HSPCs and γ H2AX expression by flow cytometry as described in the Experimental

Procedures. (E-F) Increased donor reconstitution and number of *Id1*^{-/-} HSCs in primary recipient mice transplanted with 5-FU-BMCs. Chimeric *Id1*^{+/+} and *Id1*^{-/-} mice were treated with 5-FU (150 mg/kg mouse -2X) two weeks apart, and then BMCs were harvested 14 days after last 5-FU treatment. Pooled BMCs (1 x 10⁶/mouse) were transplanted with 1 x 10⁶ host competitor BMCs into γ -IR recipient mice. Percentage donor (CD45.2⁺) reconstitution in bone marrow, and total number of LSK Flk2⁻CD150⁺48⁻ HSCs per mouse was determined by HSPC analysis and flow cytometry, using the gating strategy shown in Figure S2B, 12 weeks after BMT (n=5 mice/group).

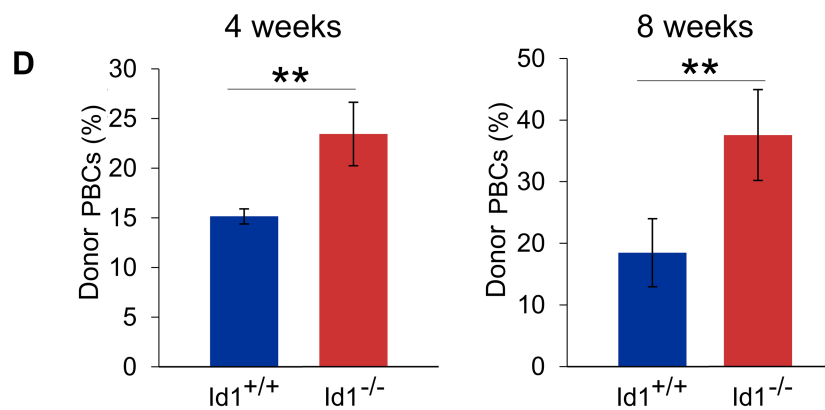
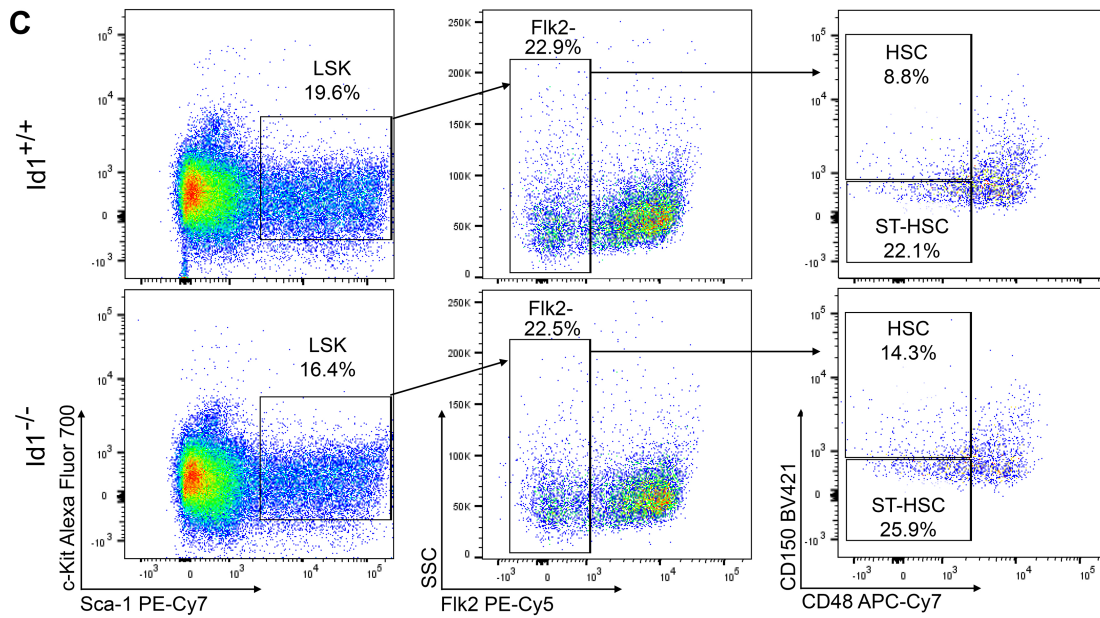
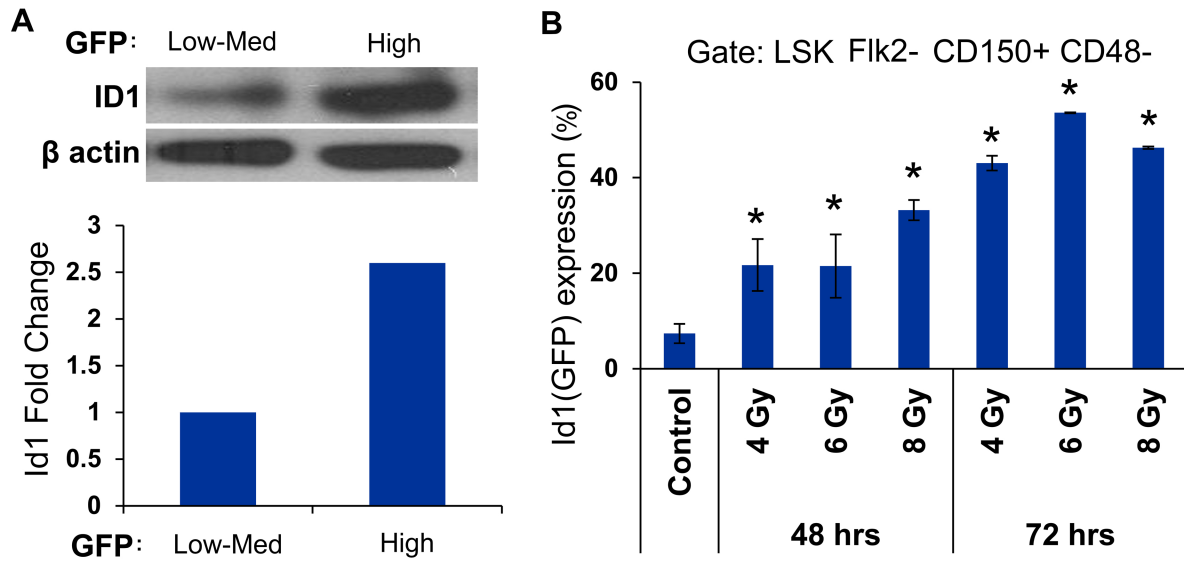
For all graphs, data are presented as mean \pm SD, n=5, * P < 0.05. ** P < 0.01.



Supplemental Figure 5

Figure S5. Related to Figure 3, ROS expression, mitochondrial biogenesis and mitochondrial stress in *Id1*^{-/-} and *Id1*^{+/+} HSCs under homeostasis.

BMCs were harvested from young (2 month), middle age (12 month) and aged (2 year) *Id1*^{-/-} and *Id1*^{+/+} mice (n=5 mice/group). HSPCs were analyzed for (A) ROS expression, (B) mitotraker green expression, and (C) TMRM expression by flow cytometry according to the methods outlined in the Experimental Procedures, using the gating strategy shown in Figure S1D. Flow cytometry plots of TMRN and mitotraker green expression in *Id1*^{-/-} and *Id1*^{+/+} HSCs are shown for aged mice. For all graphs, data are presented as mean \pm SD, n=5, * P < 0.05, ** P < 0.01, *** P < 0.001, and are representative of two independent experiments.

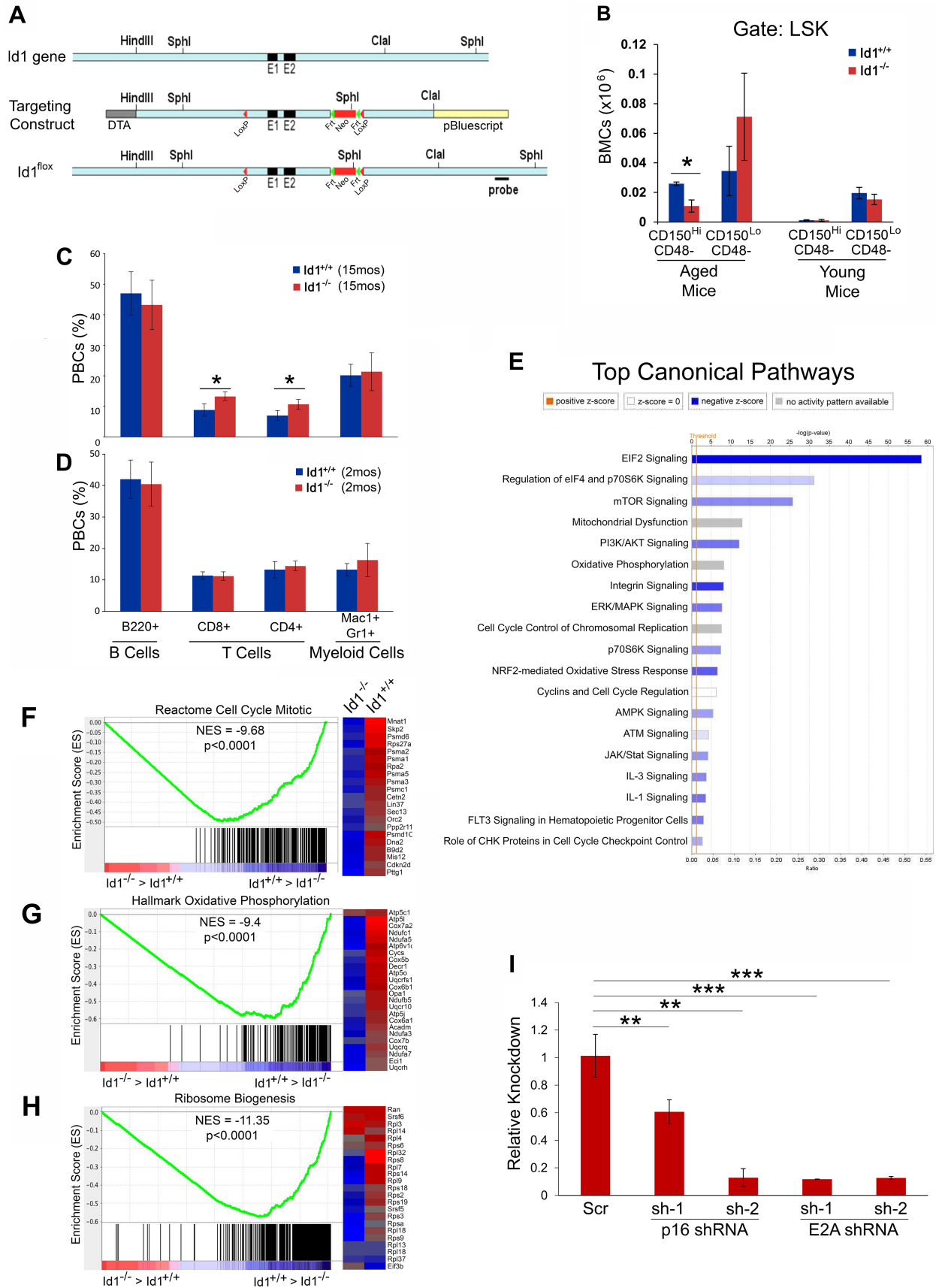


Supplemental Figure 6

Figure S6. Related to Figure 4, Expression of Id1 and radiation induced Id1(GFP) expression *in vivo*.

(A) GFP expression accurately reports Id1 expression in BMCs. LSM BMCs from $Id1^{GFP/+}$ reporter mice were cultured ($3 \times 10^5/ml$) in StemSpan media containing SCF/TPO/IFN γ for 36 hours. GFP^{Hi} and GFP^{Lo/Med} expressing cells in these cultures were isolated by FACS, and protein cell lysates were prepared for analysis of Id1 protein expression by Western blot analysis according to the Experimental Procedures. Upper panel shows a representative blot and lower panel depicts densitometric analysis of Western blot. (B) $Id1(GFP)$ expression is induced in HSCs after γ -IR. BMCs were harvested from $Id1^{GFP/+}$ reporter mice 48 and 72 hours after 4 Gy, 6 Gy, and 8 Gy γ -IR, and $Id1(GFP)$ expression levels in HSCs (LSK Flk2- CD150⁺ CD48⁻) were determined by flow cytometry using the gating strategy shown in Figure S2B. (C) Gating strategy for HSC analysis by flow cytometry for $Id1^{-/-}$ and $Id1^{+/+}$ LSK cultured cells. LSK cells were isolated by FACS from $Id1^{+/+}$ and $Id1^{-/-}$ BMCs, and then cultured in serum free media with 5 factors (SCF/TPO/FGF1/IGF2/Angpt2) for 6 days, and then analyzed for HSCs by flow cytometry. (D) LSK cells were isolated by FACS from $Id1^{+/+}$ and $Id1^{-/-}$ BMCs, and cultured in serum free media with 5 factors (SCF/TPO/FGF1/IGF2/Angpt2) for 6 days, after which, cultured LSK cells (3×10^4 cells) were co-transplanted with 3×10^5 competitor CD45.1⁺ BMCs into 10 Gy γ -IR recipient mice. Donor reconstitution was monitored in PBCs 4 and 8 weeks after BMT by flow cytometry.

For all graphs, data are presented as mean \pm SD, n=5, * P < 0.05, ** P < 0.01, *** P < 0.001.



Supplemental Figure 7

Figure S7. Related to Figure 6 and 7, HSC aging in *Tie2;Id1^{-/-}* and *Tie2;Id1^{+/+}* mice, and molecular quiescence of *Id1^{-/-}* HSCs.

(A) Schematic representation of *Id1^{fl/fl}* mice, where exons 1 and 2 are flanked by LoxP sites. We bred *Id1^{fl/fl}* mice to male *Tie2-Cre* transgenic mice, which intrinsically deletes *Id1* in HSCs and endothelial cells, but not other cells in the hematopoietic microenvironment.

(B) Increased numbers of *Id1^{-/-}* CD150^{Hi} CD48⁻ HSCs in aged mice. BMCs were harvested from aged (24 month) *Tie2;Id1^{-/-}* and *Tie2;Id1^{+/+}* mice and HSPCs were analyzed by flow cytometry as described in Experimental Procedures, using the gating strategy shown in Figure S1D. Total numbers of CD150^{Hi} CD48⁻ and CD150^{Lo} CD48⁻ HSCs were determined in aged (n=3) and young (n=5) *Tie2;Id1^{-/-}* and *Tie2;Id1^{+/+}* mice using HSC frequency and total BM cellularity.

(C-D) Increased T cell repopulation in aged *Tie2;Id1^{-/-}* and *Tie2;Id1^{+/+}* mice. Peripheral blood was collected from young (2 months) and aged (15 months) *Tie2;Id1^{-/-}* and *Tie2;Id1^{+/+}* mice, and then lysed with ACK buffer to remove red blood cells. Percentage B cells (B220⁺), T cells (CD4⁺ and CD8⁺) and neutrophils (Mac-1⁺Gr-1⁺) in the remaining cells was determined by flow cytometry as described in the Experimental Procedures (n=5 mice/group). Data are presented as mean ± SD, and are representative of two independent experiments. For all graphs, data are presented as mean ± SD, n=5, * P < 0.05. (E) IPA analysis of differentially expressed genes in *Id1^{-/-}* and *Id1^{+/+}* HSCs from primary BMT recipient mice (Table S1). The significant canonical pathways affected by this analysis are indicated on the y-axis. Bar colors indicate predicted pathway *activation* (orange), and predicted inhibition (blue) (z-score). The significance values for the canonical pathways is calculated by Fisher's exact test (-log of p-value). The molecular and cellular functions affected by the indicated pathways are all decreased in *Id1^{-/-}* HSCs. (F) GSEA analysis of differentially expressed genes in *Id1^{-/-}* and *Id1^{+/+}* HSCs shows an enrichment

of Reactome Cell Cycle Mitotic genes indicating a significant reduction in cell cycle regulated genes in *Id1*^{-/-} HSC after BMT compared to *Id1*^{+/+} HSCs, **(G)** an enrichment of Hallmark Oxidative Phosphorylation genes indicating a significant reduction in genes that regulate mitochondrial oxidative phosphorylation in *Id1*^{-/-} HSCs after BMT compared to *Id1*^{+/+} HSCs, **(H)** an enrichment of Ribosome Biogenesis genes demonstrating a significant reduction in genes that regulate ribosomal function in *Id1*^{-/-} HSCs after BMT compared to *Id1*^{+/+} HSCs. **(I)** *p16* and *E2A* expression are reduced by lentiviral-mediated knockdown in HSC expansion cultures *in vitro*. RNA was purified from cells grown in HSC expansion cultures, and *p16* and *E2A* expression was determined by Q-RT-PCR as described in the experimental procedures.